Korean J. Chem. Eng., **19**(1), 46-51 (2002)

Studies on the Analyses for the Scale of FGD Process

Kyeongsook Kim†, Sukran Yang, Haeran Song and Heemoon Eum

Radiation & Environment Group, Nuclear Power Laboratory,
KEPRI, 103-16, Munji, Yusung, Daejeon 305-345, Korea
(*Received 2 April 2001 • accepted 6 September 2001*)

Abstract−During the period of preventive maintenance of the Ulsan power plant, the scale was sampled from riser pipes, sparger pipes and other important parts in the FGD facilities. Various analyses such as concentration analysis, surface morphology, and crystal structure have been performed on the scale sample. The riser pipe scale was a gypsum dihydrate form. The sparger pipe scale was different from two units, namely, gypsum dihydrate form was obtained from that of unit 6; on the other hand, 1 to 1 ratio of gypsum dihydrate form and anhydrate form was elucidated from that of unit 4. Next, the analyses of GCP spray nozzle head scale, gas-cooling zone scale, and BUF inlet duct scale were focused on the effect of base material. On the basis of the analytical results, we expect to elucidate the formation process of the scale, and finally to improve the FGD process.

Key words: FGD Scale, Sparger Pipe, Riser Pipe, GCP Spray Nozzle Head, Gas-Cooling Zone

INTRODUCTION

Studies on the flue gas desulfurization (FGD) process for the gas emitted from power plants have attracted considerable attention since the sulfur compound in the gas has been known to bring about serious environmental problems. In the Korea Electric Power Corporation (KEPCO), many FGD facilities for eliminating SO_x are currently operating and some of them are under construction now. In the FGD facilities of all power plants in KEPCO, limestone is used as an absorbent. In those facilities, a forced oxidation method is also applied to produce gypsum as a byproduct. The chemical reactions--absorption, oxidation, neutralization, and crystallization--occurring in the FGD facilities are shown in Scheme 1 [Hanzel and Laseke, 1980; Lee et al., 2000].

The absorbers for 22 units are spray tower types, which are spraying limestone slurry in influxing flue gas. On the other hand, the residues for 7 units including Ulsan units 4, 5, and 6 are bubble types, which are spraying a flue gas in absorbing solution. The bubble type, which has been developed by Chiyoda Corporation, has some advantages. For instance, in the bubble type the process is very simple, the absorbents can be highly utilized, and the concentration of wastewater is very low. This is because all the reactions, such as absorption, oxidation, and neutralization, are occurring in one reactor. However, the bubble type also has some disadvantages in that gas pressure is decreased, so actual application cases are very rare to large-scale power plants.

Absorption	$SO_2+H_2O \leftrightarrow H_2SO_3$
↓	
Oxidation	$H_2SO_3+\frac{1}{2}O_2 \rightarrow H_2SO_4$
↓	
Neutralization	$CaCO_3+H_2SO_4 \rightarrow CaSO_4+CO_2+H_2O$
↓	
Crystallization	$CaSO_4+2H_2O \rightarrow CaSO_4 \cdot 2H_2O$

Scheme 1. Chemical reactions in FGD process.

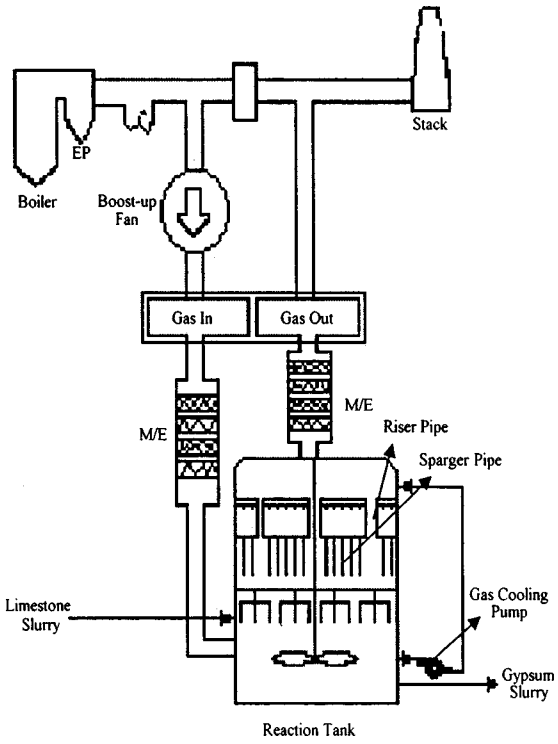

Fig. 1. Schematic diagram of FGD at Ulsan power plant.

Fig. 1 shows a schematic diagram of the bubble-type absorber, located in Ulsan power plant. The flue gas, which has passed through the electrostatic precipitator (EP), goes to the gas gas heater (GGH), the duct-cooling part named the gas-cooling zone, and then flows in the sparger pipe located at the middle layer of jet bubbling reactor (JBR). The SO_2 of flue gas, which was passed through the sparger pipe, falls down into the reaction tank, and it is reacted with the limestone slurry. It is also converted into gypsum dihydrate in the tank.

†To whom correspondence should be addressed.
E-mail: kskim@kepri.re.kr

The treated flue gas rises to the upper JBR through the riser pipes, and then passes through the mist eliminator (M/E), GGH. Finally it is exhausted to the atmosphere. JBR is also utilized to cool the flue gas by spraying gypsum slurry to the gas-cooling duct by using the gas-cooling pump (GCP).

During the period of preventive maintenance on January and December 2000, the scale was sampled from the riser pipe, sparger pipe, and other important parts in the FGD facilities, respectively. Various analyses such as surface morphology, crystallography, and concentration analysis have been performed on the scale sample. On the basis of the analytical results, we expect to contribute to improving the FGD process.

EXPERIMENTAL

1. Reagent and Equipment

The standard solutions for the concentration analysis were purchased from Perkin-Elmer Corporation. The concentration of each component was determined from ICP-AES (model: Spectro-P, maker: Spectro Co.). The surface morphology was observed by using SEM (model: JSM 6400, maker: Jeol Co.). The crystal structure was identified by using XRD (model: Ultima+2200, maker: Rigaku Co.). The purity of gypsum was determined from the amount of combined water measured by TGA (model: SDT 2960, maker: TA instruments). The purities of calcium carbonate and magnesium carbonate were determined from the amounts of CO_2 and Mg, respectively.

2. Pre-treatment and Experimental Method

The bulk-type scale, collected from the plants, was ground by using a mortar and pestle. It was meshed to about 74 μm size, dried at the temperature below 45 °C, and then kept in a desiccator. Gypsum dihydrate ($CaSO_4 \cdot 2H_2O$), SiO_2, Al_2O_3, Fe_2O_3, $CaCO_3$ and $MgCO_3$ were analyzed by the methods as described below. $CaSO_3 \cdot \frac{1}{2} H_2O$ was analyzed by the KS L 9003 method. The scale, sampled from boost-up fan (BUF) inlet duct, was analyzed by using ICP-AES after the carbon component in the scale was eliminated by nitric acid and perchloric acid. This is because the sample contains a large amount of ash [KS, 1996; Brenner et al., 1999; Caroli et al., 1999; Kanicky et al., 1997; Lau et al., 2000; Mao et al., 1997; Park et al., 2000; Rodushkin et al., 2000; Thompson, 1997; Wei et al., 1999].

2-1. $CaSO_4 \cdot 2H_2O$ (Gypsum Dihydrate)

The residue mass was measured with increasing temperature at a rate of 10 °C/min from room temperature to 250 °C under nitrogen atmosphere. The amount of combined water was determined from the residue mass in the 90-200 °C range. The amount of $CaSO_4 \cdot 2H_2O$ was also determined by multiplying a factor of 4.778 [ASTM 1985; Kim, 2000b].

2-2. SiO_2+Insolubles, Al_2O_3, Fe_2O_3 and MgO

Three grams of sample was dissolved in acids and filtered, and then put in a 1 L-volumetric flask. The concentrations of Al, Fe, and Mg were measured by using ICP-AES. They were also converted to oxidized forms such as Al_2O_3, Fe_2O_3, and $MgCO_3$. The insoluble material was filtered, and ignited at 850 °C for 2 hours. Then the weight of the residue, SiO_2+insoluble, was measured [KS, 1996].

2-3. $CaCO_3$

The weight of total CO_2 was determined by CO_2 measuring equipment of KS L 9003. The weight of CO_2 in magnesium carbonate was determined from the amount of Mg in magnesium carbonate. In this case, the residual CO_2 was considered as $CaCO_3$ [KS, 1996].

2-4. Surface Morphology

To observe the microstructure of the scale during the formation and growth of gypsum crystal, the polished and gold-coated scales were closely examined.

2-5. Crystal Structure

The crystal structure of the scale was analyzed as a powder form by XRD analysis.

RESULTS AND DISCUSSION

1. Stereozoom Microscope Observation

Meaningful information could not be obtained from the observation of a stereozoom microscope of most scales. However, a few scales were observed to be separated into two layers in the stereozoom microscope. For example, the outer scale in the riser pipe was observed as a tube shape with a constant thickness. Thus, the scale could be separated into two layers; a thick, loose, and bright layer named as a pale part and the other named as a dark part. Therefore, the experimental analysis was performed on two separate layers. The microscopic features for the inner scale in the sparger pipe from unit 4 are shown in Fig. 2. Generally, the outer scale in the riser pipe looks like a soft gypsum. On the other hand, the inner scale in the sparger pipe relatively looks hard and tough [Kim et al., 2000a].

2. SEM Observation

Generally, most of the scales sampled from FGD facility were observed as gypsum dihydrates. Fig. 3 shows the SEM observations for the outer scale in the riser pipe. As shown in Fig. 3(a), a pale part shows a relatively loose and irregular crystalline structure, and the size of crystal is about 40 μm. This corresponds to a typical gypsum dihydrate produced from FGD facilities. On the contrary, a dark part is observed as a relatively dense, packed and layered structure in Fig. 3(b) [Kim et al., 2000a; Lee et al., 2000; Wolfgang, 1985].

3. Crystalline Structure

The XRD patterns for the scale sampled from each site are listed in Table 1. The outer scales in the riser pipe, sampled from unit 4 on January and December 2000, were mostly identified as gypsum dihydrate. Small amounts of muscovite and brushite were also identified. On the other hand, most of inner scales in the sparger pipe,

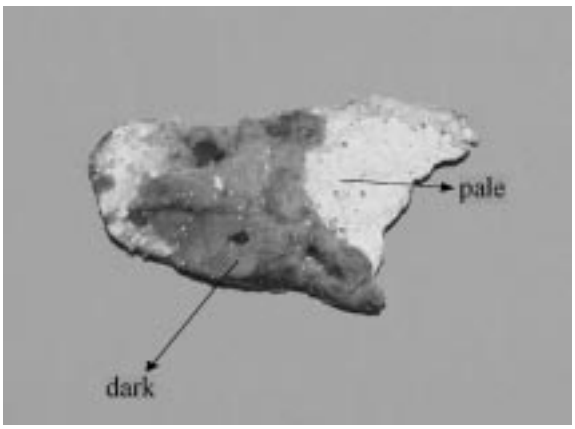

Fig. 2. Stereozoom microscope feature of sparger pipe scale.

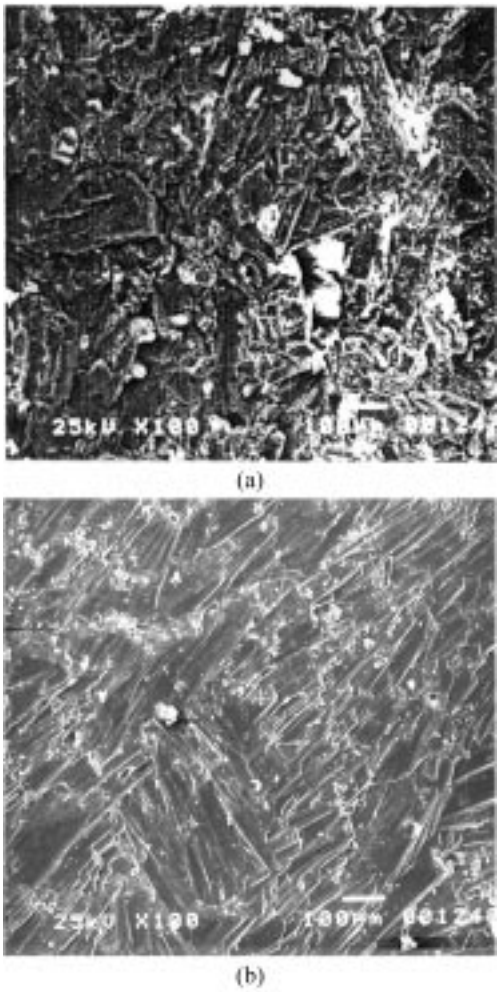

Fig. 3. SEM features of riser pipe scale, (a) pale part (b) dark part.

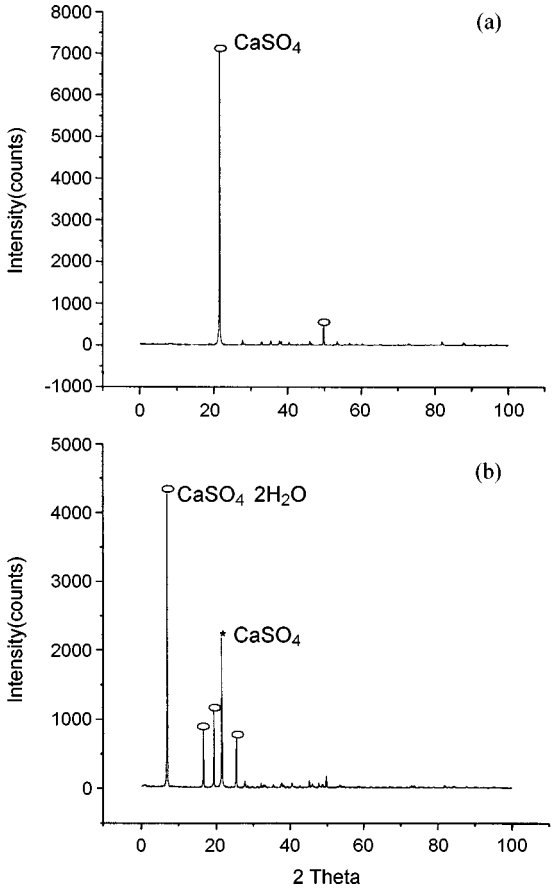

Fig. 4. XRD spectra of sparger pipe scale, (a) pale part (b) dark part.

sampled from unit 4 and 5 on January 2000, were identified as gypsum dihydrate [Lee et al., 2000].

The XRD spectra of the scale, sampled from unit 4 on December 2000, are shown in Fig. 4. As depicted in Fig. 4(a), the pale part shows a gypsum anhydrite structure. The dark part shows both gypsum dihydrate and gypsum anhydrite as shown in Fig. 4(b).

The scales in the GCP spray nozzle head, sampled from unit 6 on January 2000, were identified as gypsum dihydrate, SiO_2 and muscovite. Since the SiC structure corresponding to the nozzle head base material could not be seen due to the excessive amount of gypsum dihydrate, the XRD analysis was performed again after eliminating gypsum dihydrate by using 0.1N-EDTA. As depicted in Fig. 5,

Table 1. Results of XRD

Sample	Unit (Date)	Crystallographic structures
Riser pump	# 4(2000. 1)	gypsum, syn($CaSO_4 \cdot 2H_2O$), muscovite
	# 4(2000. 12)	pale: gypsum, syn($CaSO_4 \cdot 2H_2O$), brushite
		dark: gypsum, syn($CaSO_4 \cdot 2H_2O$), brushite
Sparger pipe	# 6(2000. 1)	gypsum, syn($CaSO_4 \cdot 2H_2O$), muscovite
	# 5(2000. 1)	pale: gypsum, syn($CaSO_4 \cdot 2H_2O$), muscovite
		dark: gypsum, syn($CaSO_4 \cdot 2H_2O$), muscovite
	# 4(2000. 12)	pale: anhydrite, syn($CaSO_4$)
		dark: gypsum, syn($CaSO_4 \cdot 2H_2O$), anhydrite, syn($CaSO_4$), brushite
GCP spray nozzle	# 6(2000. 1)	gypsum, syn($CaSO_4 \cdot 2H_2O$),
		quarts, syn(SiO_2), muscovite
Gas cooling zone	# 6(2000. 1)	anhydrite, syn($CaSO_4$), silicone oxide(SiO_2)
BUF inlet duct	# 4(2000. 12)	iron sulfate, $Fe_2(SO_4)_3$,
		gunningite, syn($ZnSO_4 \cdot H_2O$)

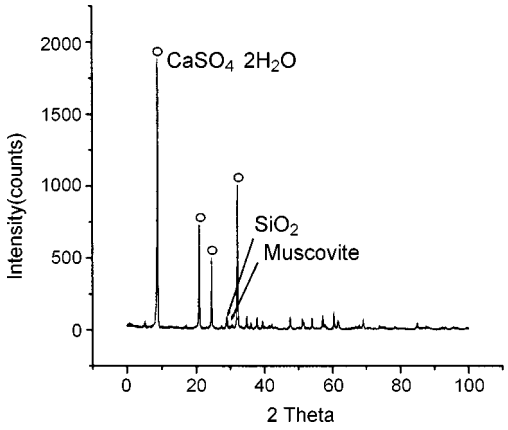

Fig. 5. XRD of spray nozzle scale.

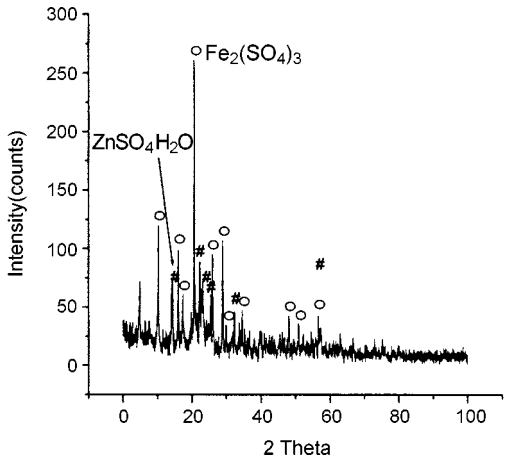

Fig. 6. XRD of BUF inlet duct scale.

the structure of SiC could not be observed.

The scales in the gas-cooling zone, sampled from unit 6 on January 2000, were identified as gypsum anhydrite and SiO_2 [Reifenstein et al., 1997].

As shown in Fig. 6, the XRD spectra of BUF inlet duct scale, sampled from unit 4 on December 2000, were identified as $Fe_2(SO_4)_3$ and $ZnSO_4$ which were produced from the reactions of Fe and Zn with SO_4 due to the oxidation of SO_2 emitted from duct.

4. Concentration Analysis

4-1. Outer Scales in the Riser Pipe

Table 2 lists the results for the concentration analysis of the outer scales in the riser pipe, sampled from unit 4 on January and December 2000. Gypsum dihydrate was obtained from the same unit as a reference. Table 2 shows that the concentration of gypsum dihydrate is higher than that of the reference, and the concentration of unreacted limestone in the scale is lower than that of unreacted limestone in the reference.

Table 2. Concentration analysis of riser pipe scale (unit: wt%)

Items \ Sample	2000. 1	2000. 12		Gypsum (2000. 1)	Gypsum (2000. 12)
		Pale part	Dark part		
$CaSO_4 \cdot 2H_2O$	96.52	91.88	96.75	95.18	94.32
$CaSO_3 \cdot \frac{1}{2}H_2O$	0.07	0.06	0.06	0.01	0.05
SiO_2+insoluble	1.82	4.92	0.16	2.45	1.95
$Al_2O_3+Fe_2O_3$	0.53	0.32	0.51	0.37	0.52
$CaCO_3$	0.47	2.32	2.16	1.28	2.76
$MgCO_3$	-	0.02	0.02	-	0.46

On the other hand, the outer scale in the riser pipe, sampled on December 2000, was analyzed upon two separate parts. The concentration of gypsum dihydrate of a dark part was higher than that of a pale part. The difference in concentration of gypsum dihydrate for two parts is about 5%, and this corresponds to the concentration of SiO_2+insoluble.

4-2. Inner Scales in the Sparger Pipe

Table 3 lists the results for the concentration analysis of the inner scales in the sparger pipe, sampled from units 5 and 6 on January 2000. Most of the scales were gypsum dihydrate, and the concentration of gypsum dihydrate from unit 5 was 2% lower than that of reference. Meanwhile, the concentration of gypsum dihydrate from unit 6 was determined to be similar with that of the reference.

The inner scale in the riser pipe, sampled from unit 4 on December 2000, shows a very consistent result in that the concentration of $CaSO_4$ (anhydrite form) of the pale part is 96.60% and those of $CaSO_4$ (anhydrite form) and $CaSO_4 \cdot 2H_2O$ (dihydrate form) of dark part are 48.32% and 48.00%, respectively. Compared to the reference, the concentrations of $MgCO_3$ and $CaCO_3$ in both samples are remarkably reduced due to the repeated reactions of limestone with the flue gas for a long time.

The formation of unexpected gypsum anhydrite could be explained by the conversion mechanism and the chemical process. First, there are three different types of reactions named as I, II, and III for gypsum anhydrite as shown in Fig. 7. However, reaction type I can only occur over 1,180 °C, and the temperature of FGD fa-

Table 3. Concentration analysis of sparger pipe scale (unit: wt%)

Items \ Sample	# 6 (2000. 1)	# 5 (2000. 1)		# 4 (2000. 12)	
		Pale part	Dark part	Pale part	Dark part
$CaSO_4 \cdot 2H_2O$	94.17	92.84	92.84	-	48.00
$CaSO_3 \cdot \frac{1}{2}H_2O$	0.11	0.18	0.05	0.04	0.04
$CaSO_4$	-	-	-	96.60	48.32
SiO_2+insoluble	3.69	2.29	2.51	1.76	2.83
$Al_2O_3+Fe_2O_3$	1.23	2.01	2.11	0.20	0.18
$CaCO_3$	0.83	0.24	0.25	0.36	0.27
$MgCO_3$	0.35	0.81	0.70	0.06	0.03

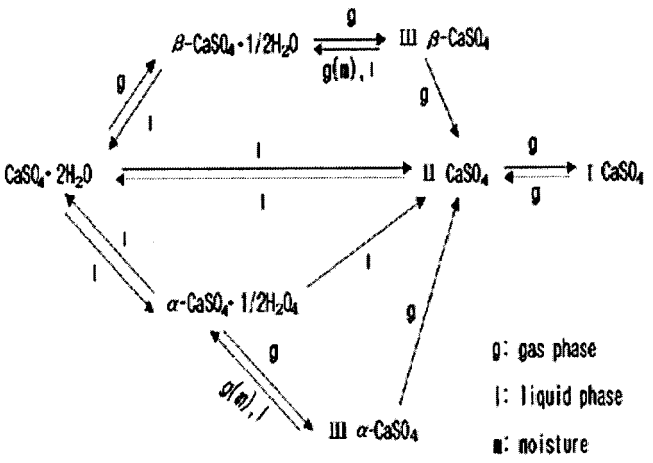

Fig. 7. Conversion process of gypsum.

cilities cannot be reached at this high temperature. Thus, reaction type I should be excluded. Reaction type III is not expected to be obtained as a pure state either because gypsum is supposed to be easily combined with moisture, and converted into gypsum hemihydrate. Therefore, the possibility of reaction type III is expected to be very low. This is because 97% purity of the gypsum anhydrite is obtained in this case. As a result, the possibility of reaction type II looks very high. Besides, a one-to-one ratio for dihydrate and anhydrite of a dark part is also deduced in that anhydrite of type II is directly converted into dihydrate without a hemihydrate form. Thus, anhydrite of type III is unstable, and easily converts into hemihydrate. Second, anhydrite is expected to be formed by the chemical process of gypsum as previously mentioned in Scheme 1. If the fourth step, crystallization, is not completely proceeding gypsum anhydrite can be produced. The inner temperature might play an important role in this process. If the inner temperature in the sparger pipe is not greatly increased, this explanation is more reasonable compared to the previously mentioned conversion processes [Wolfgang, 1985].

4-3. Scale in the GCP Spray Nozzle Head

The results for the concentration analysis of GCP spray nozzle head scale, sampled from unit 6 on January 2000, are shown in Table 4. The contents of gypsum dihydrate are determined to be slightly lower, 87.49%, than those in the sparger pipe. On the other hand, the contents of SiO_2+insoluble and Al_2O_3+Fe_2O_3 are measured to be slightly higher. The gray color of the scale is caused by 0.82% of carbon. As the concentrations of Si, Fe and Al are higher than those of reference, the effect of base material on the scale was investigated and the results are shown in Table 4.

Table 4. Concentration analysis of GCP spray nozzle scale

(unit: wt%)

Items \ Sample	# 6 scale (2001. 1)	Material (SiC)	Gypsum (2001. 1)
$CaSO_4 \cdot 2H_2O$	87.49	-	94.32
$CaSO_3 \cdot \frac{1}{2} H_2O$	0.10	-	0.05
$CaCO_3$	0.12	-	2.76
$MgCO_3$	0.60	-	0.46
SiO_2+insoluble	6.75	3	1.95
Al_2O_3	2.97	2.7	0.52
Fe_2O_3	0.71	0.3	(Al_2O_3+Fe_2O_3)
SiC	-	73	-
Si_3N_4	-	21	-
C	0.82	-	-

Table 5. Concentration analysis of gas cooling zone and BUF scale

(unit: wt%)

Items \ Sample	# 6 Gas cooling zone (2000. 1)	# 4 BUF inlet duct (2000. 12)	Alloy C-276 cast 33588	Ash (reference)
Cr	0.93	0.02	15.75	0.01
Ni	6.54	0.76	58.55	3.53
Mn	-	0.11	0.29	0.01
Mo	1.16	0.02	16.00	0.03
Cu	-	0.02	0.04	0.01
Fe	0.95	17.63	5.42	3.39
P	-	0.01	0.005	-
W	-	-	3.33	-
Co	-	-	0.04	-
V	-	1.79	0.20	4.38
C	-	4.48	0.004	60.45
S	18.50	15.32	0.002	8.95
SiO_2+insoluble	0.94	1.02	0.04	0.02
Al	0.28	0.22	-	0.08
Na	-	0.20	-	1.14
Ca	10.09	0.13	-	0.20
Zn	-	4.58	-	0.05

4-4. Scale in the Upper Gas Cooling Zone and BUF Inlet Duct

The scales in the gas-cooling zone, sampled from unit 6 on January 2000, turned out to be ash, gypsum dihydrate, and base material. In order to identify the compositions, the experimental analyses were performed after eliminating carbon. As shown in Table 5, one of the characteristic properties is that the concentration of SO_3 is very different from that of ash. This is because more SO_3 is added from gypsum dihydrate. Besides, the concentration of Fe, Ni, Cr, and Mo corresponding to the base material (C-276) is higher than that of ash. Therefore, it is concluded that the scale contains very little base material (C-276).

The results of concentration analysis of the scale in the BUF inlet duct, from unit 4 on December 2000, are shown in Table 5. The constituents, which came from the base material, Cr, Ni and Mo, were not observed.

CONCLUSION

First, the outer scale in the riser pipe, sampled from unit 4 on January 2000, turned out to be composed of a typical FGD gypsum, gypsum dihydrate, and the content of gypsum dihydrate is very high. Meanwhile, the scale from the same unit on December 2000 is apparently separated into two parts, that is, the pale and dark parts. A pale part has a relatively loose and irregular crystalline structure, but a dark part has a relatively dense, packed, and layered structure. The difference in the concentration of gypsum dihydrate for

two parts is about 5% and this is caused by the amounts of SiO_2+ insoluble. The scale does not have an effect on the base material, super austenitic stainless steel; therefore, if an operational problem occurs, it can be fixed with dissolving the scale by chelating agents such as EDTA, glycerol and sugar solution.

Second, the inner scale in the sparger pipe, sampled from unit 6 on January 2000, turned out to be almost the same as with gypsum dihydrate in the reaction tank. On the other hand, the scale, from the same unit 4 on December 2000, can apparently be separated into two parts, and the type of gypsum is also different from the other. A pale part is composed of 97% of gypsum anhydrite, and a dark part is composed of one-to-one ratio of gypsum dihydrate (48%) and gypsum anhydrite (48%). These unexpected results can be explained by two different procedures. One is the conversion mechanism involving anhydrite, hemihydrate, and dihydrate form, and the other is the chemical process of gypsum formation related to absorption, oxidation, neutralization, and crystallization. Considering that the base material in the sparger pipe is PVC, and the inner temperature of sparger pipe cannot be increased over 100 °C due to GGH, the latter explanation looks more reasonable. Further studies will be focused on explaining these results. In particular, a considerable amount of unexpected anhydrite was observed, and the content of gypsum dihydrate from unit 4 decreased as time passed in the year 2000. For these reasons, we performed a preventive maintenance in December 2000.

Third, in the case of the scale in the GCP spray nozzle, the experimental analysis was focused on the effects of base material, silicone carbide (SiC). Most of the scale turned out to be gypsum dihydrate and ash, but silicone carbide was not observed. On the basis of this analytical result, it is concluded that the part scale does not have an effect on the base material.

Fourth, the analyses of the scale in the gas-cooling zone were also focused on the effects of the base material, alloy C-276. Since the concentrations of Fe, Ni, Cr, and Mo corresponding to alloy C-276 are higher than those of ash, the scale contains a small amount of alloy C-276. Furthermore, gypsum anhydrite was also observed. As the scales in the gas-cooling zone can affect the base material, particular caution should be required. If scales are attached to this part, detaching methods to minimize the effects of base material should be considered.

Fifth, the analyses of BUF inlet duct scale were focused on the effects of base material, alloy C-276 and heavy oil used as a fuel. Fe, S, Zn, and C are major elements, and Cr, Ni and Mo are not involved in this case; therefore, this scale does not have an effect on the base material. Two compounds, $Fe_2(SO_4)_3$ and $ZnSO_4$ were identified in the scale, and these compounds are expected to be produced from the reactions of Fe and Zn with SO_4 due to the oxidation of SO_2 emitted from duct.

REFERENCES

ASTM C471-76, "Chemical Analysis of Gypsum and Gypsum Products," 1 (1985).

Brenner, I. B., Vats, S. and Zander, A. T., "New CCD Axially Viewed ICP Atomic Emission Spectrometer for Simultaneous Multi-element Geoanalysis. Determination of Major and Minor in Silicate Rocks," *J. Anal. Atomic Spectrometer*, **14**, 1231 (1999).

Caroli, S., Forte, G. and Iamiceli, A. L., "ICP-AES and ICP-MS Quantification of Trace Elements in the Marine Macroalga Fucus sample, a New Candidate Certificate Reference Material," *Microchem. J.*, **62**, 244 (1999).

Hanzel, D. S. and Laseke, B. A., "Construction Materials for Wet Scrubbers," EPRI CS1-1736, Mar. (1980).

Kanicky, V. and Mermet, J.-M., "Selection of Internal Standards for the Determination of Major and Minor Elements in Silicate Rocks and Limestone by Laser Ablation Inductively Coupled Plasma Atomic Emission Spectrometry," *Applied Spectroscopy*, **51**, 332 (1997).

Kim, K., Park, H., Lee, T. and Jeong, N., "Analysis of the Clinker Formed in Circulating Fludized Bed Boiler," *Analytical Science & Technology*, **13**, 5 (2000a).

Kim, K., Yang, S., Park, H. and Lim, C., "The Comparison of Analytical Methods for Gypsum and Gypsum Slurry," *Analytical Science & Technology*, **13**, 158 (2000b).

KS L9003-1996, "Method for Chemical Analysis of Gypsum," KS, 1 (1996).

Lau, O.-W., Lam, L. and Luk. S.-F., "Analysis of Siliceous Materials and Coal by Atomic Absorption Spectrophotometry with Fusion for Sample Decomposition," *Talanta*, **51**, 1009 (2000).

Lee, S., Kim, K., Yang, S. and Jeong, N., "Analysis of the Scale Formed in GGH," *HWAHAK KONGHAK*, **38**, 882 (2000).

Mao, X., Chan, W. T. and Russo, R. E., "Influence of Sample Surface Condition on Chemical Analysis Using Laser Ablation Inductively Coupled Plasma Atomic Emission Spectroscopy," *Applied Spectroscopy*, **51**, 1047 (1997).

Park, H., Kim, K., Yang, S. and Lee, G., "Studies on the Analytical Methods of Coal Ash," *J. Korean Chem. Soc*., **44**, 563 (2000).

Reifenstein, A. P., Kahraman, H., Coin, C. D. A., Calos, N. J., Miller, G. and Uwins, P., "Behavior of Selected Minerials in an Improved Ash Fusion Test: Quarts, Potassium Feldspar, Kaolinite, Illite, Calcite, Dolomite, Siderite, Pyrite and Apatite," *Fuel*, **78**, 1449 (1999).

Rodushkin, I., Axelsson, M. D. and Burman, E., "Multieliment Analyses of Coal by ICP Techniques Using Solution Nebulization and Laser Ablation," *Talanta*, **51**, 743 (2000).

Thompson, M., "Handbook of Inductively Coupled Plasma Spectrometry," 2nd. Ed., Champman & Hall, 93 (1989).

Torigai, M., Ouyang, T., Iwashima, K., Osako, M. and Tanaka, M., "Studies on Microwave Digestion Procedure for the Simultaneous Multielement Determination of Arsenic, Antimony, Chromium, Cadmium, Nickel, and Lead in Municipal Waste Incineration Fly Ash by ICP-AES," *BUNSEKI KAGAKU*, **46**, 401 (1997).

Wei, R., Ikeda, K., Takeuchi, A., Jomen, K., Yamanaka., K., Sawatari, H. and Haraguchi, H., "Multielemental Determination of Major-to-ultratrace Elements in Lake Sediment Reference Materials by ICP-AES and ICP-MS," *BUNSEKI KAGAKU*, **48**, 365 (1999).

Wolfgang Gerhartz, "Calcium Sulfate," Ullmann's Encyclopedia of Industrial Chemistry, Deerfield Beach, FL, VCH, **4A**, 555 (1985).